

RL-GSBridge: 3D Gaussian Splatting Based Real2Sim2Real Method for Robotic Manipulation Learning

Yuxuan Wu*, Lei Pan*, Wenhua Wu, Guangming Wang, Yanzi Miao, and Hesheng Wang

Abstract—Sim-to-Real refers to the process of transferring policies learned in simulation to the real world, which is crucial for achieving practical robotics applications. However, recent Sim2Real methods either rely on a large amount of augmented data or large learning models, which is inefficient for specific tasks. In recent years, radiance field-based reconstruction methods, especially the emergence of 3D Gaussian Splatting, making it possible to reproduce realistic real-world scenarios. To this end, we propose a novel real-to-sim-to-real reinforcement learning framework, RL-GSBridge, which introduces a mesh-based 3D Gaussian Splatting method to realize zero-shot sim-to-real transfer for vision-based deep reinforcement learning. We improve the mesh-based 3D GS modeling method by using soft binding constraints, enhancing the rendering quality of mesh models. We then employ a GS editing approach to synchronize rendering with the physics simulator, reflecting the interactions of the physical robot more accurately. Through a series of sim-to-real robotic arm experiments, including grasping and pick-and-place tasks, we demonstrate that RL-GSBridge maintains a satisfactory success rate in real-world task completion during sim-to-real transfer. Furthermore, a series of rendering metrics and visualization results indicate that our proposed mesh-based 3D Gaussian reduces artifacts in unstructured objects, demonstrating more realistic rendering performance.

I. INTRODUCTION

Learning robotic action strategies in a simulated environment and then transferring them to real-world deployment represents an ideal robotic learning model, balancing both the cost and safety of the learning process. However, a significant bottleneck in this ideal model is the reliability of sim-to-real transfer, which impacts the potential and value of the entire framework and poses substantial challenges.

With the continuous development of the sim2real field, extensive work is advancing the progress from multiple perspectives [1], [2], [3], [4]. However, most sim-to-real methods attempt to expand the distribution range of training data to cover various situations that may arise in reality or to train a highly generalized large-scale model to learn

This work was supported in part by the Natural Science Foundation of China under Grant 62225309, 62073222, U21A20480 and 62361166632. Corresponding Author: Hesheng Wang (wanghesheng@sjtu.edu.cn).

*Equal contributions

Y. Wu and H. Wang are with the Department of Automation, Shanghai Jiao Tong University, Shanghai 200240, China. (e-mail: furrygreen@sjtu.edu.cn; wanghesheng@sjtu.edu.cn)

L. Pan and Y. Miao are with the School of Information and Control Engineering, China University of Mining and Technology, Xuzhou 221100, China.

W. Wu is with MoE Key Lab of Artificial Intelligence, AI Institute, Shanghai Jiao Tong University, Shanghai 200240, China.

G. Wang is with the Department of Engineering, University of Cambridge, Cambridge CB2 1PZ, U.K. (e-mail: gw462@cam.ac.uk)

Code will soon be released at <https://github.com/FurryGreen/RL-GS-Bridge>

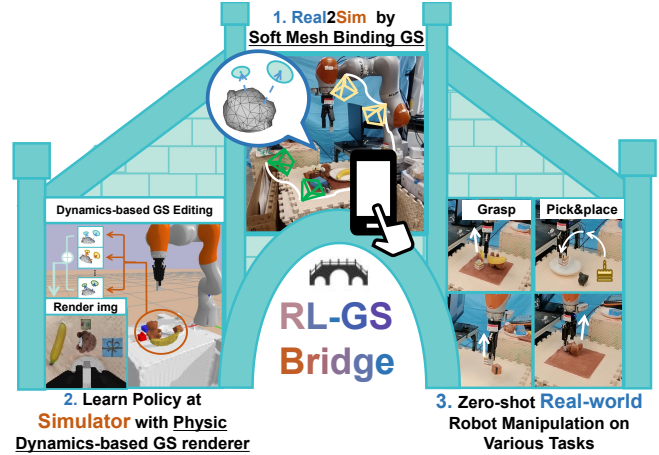


Fig. 1. Three Components of First-Person Perspective Manipulation in RL-GSBridge for Robotic Arms: (1) Real2Sim Transfer by soft mesh binding GS modeling. Given collected images from the real world, we utilize a novel soft mesh binding Gaussian models for high-quality image rendering while ensuring geometric accuracy. (2) Learn Policy at Simulator with GS Physics Dynamics-based GS Renderer. A physical dynamics-based GS editing and rendering method is proposed to enable RL algorithms to acquire realistic dynamic images. (3) Zero-shot Real-world Robot Manipulation. We directly apply the learned policy to real-world robotic manipulation tasks without any further training or fine-tuning.

knowledge for different tasks. This significantly increases the difficulty of training, and in more complex tasks, the additional training burden often leads to learning failures.

To avoid additional training burden and achieve ideal sim2real performance on specific tasks, a novel framework is needed. Recently, advances in radiance field-based reconstruction methods [5], [6], [7], [8] provide new directions for sim2real training. Based on a simple idea—using radiance field reconstruction to create a visually realistic robot training environment to achieve real2sim for vision-based policy training—can we achieve satisfactory sim2real performance? For this purpose, we design a new real2sim2real visual reinforcement learning framework, RL-GSBridge, that bridges the real-to-sim gap by 3D Gaussian splatting, as shown in Fig. 1. We utilize 3D Gaussian splatting and editing techniques, to provide a ‘virtual-reality’ simulation platform.

For vision-based robot tasks, it is crucial to avoid illusions caused by inconsistencies between visual perception and contact geometry. Thus, it is required to ensure an accurate geometric representation of the model while achieving more realistic rendering results. GaMeS [9] has drawn our attention as it is a mesh-based Gaussian Splatting (GS) method, which ensures that the optimization of the GS units is performed

within the geometric mesh model. However, it enforces the binding of Gaussians to mesh grid planes in a manner that could be considered a hard mesh binding method, thereby constraining the flexibility of GS units. To address this problem, a soft mesh binding method is proposed for Gaussian Splatting to further enhance rendering performance while providing improved modeling and editing capabilities, even for non-rigid objects.

Physics-based dynamics simulation is also a crucial and challenging aspect of sim2real. To tackle this, an off-the-shelf physics simulator is used to provide dynamic changing information. The GS editing process simultaneously updates the scene, ensuring that visual realism and the rendering results align with physical interaction processes.

We use the designed simulator with the soft mesh binding based GS models to train a robotic arm on manipulation tasks with deep reinforcement learning (DRL). The tasks include object grasping and pick-and-place. These scenarios feature various textures, geometric shapes, and patterned desktop backgrounds, simulating a range of everyday desktop manipulation scenes.

Under the RL-GSBridge framework, the policy trained in these environments demonstrates high sim2real few-shot transfer success rates. This means that the policy maintains effective performance on real-world tasks when deployed, reflecting a strong ability to generalize from simulation to actual environments.

To summarize our contributions:

- **A Novel Sim2Real RL Framework:** leveraging the high-fidelity rendering of 3D GS and the convenience of modeling scenes with only consumer-grade cameras.
- **A Soft Mesh Binding GS Modeling Method:** proposing a soft mesh binding strategy to replace the hard mesh binding baseline, enhancing the flexibility and render quality.
- **Physical Dynamics-Based GS Editing:** integrating dynamics signals from the simulator to edit 3D GS models, reflecting realistic physical robotic interactions.
- **Validation on Real Physical Robots:** testing the RL-GSBridge framework on physical robots through grasping and pick-and-place tasks in real-world scenarios with complex textures and geometries.

II. RELATED WORK

A. Sim2Real Transfer in RL

RL constructs an interactive learning model where an agent learns to maximize expected rewards through trial and error. By incorporating deep learning, DRL enhances the framework’s ability to tackle more complex tasks [10]. DRL has shown impressive performance across various domains, including games [11], finance [12], autonomous driving [13], and robotics [14]. However, most applications are confined to virtual environments due to real-world constraints related to safety, efficiency, and cost.

To improve the feasibility of deploying models in the real world, many researchers strive to bridge the gap between

simulation and reality [15]. Methods to bridge the gap include domain randomization [16] and domain adaptation [17]. Domain randomization involves varying task-related parameters in the simulation to cover a broad range of real-world conditions, while domain adaptation focuses on extracting a unified feature space from both sources. Higher-level learning methods include meta-learning [18] and distillation learning [19]. Meta-learning aims to teach robots the ability to learn new tasks, whereas distillation learning trains a student network using knowledge from expert networks.

Our approach aligns with the first category of gap-bridging methods, but with a unique twist. We use soft mesh binding GS to create highly realistic simulation environments for robot training. Typically, achieving such fidelity requires expensive 3D scanning equipment or CAD expertise. In contrast, GS models visually realistic simulation environments using only multi-view 2D images captured with consumer-grade devices.

B. Radiance Field in Robotics

Neural Radiance Fields (NeRF) [5] is a neural implicit representation technique for novel view synthesis. It optimizes the parameters through multi-view images, and allows for the synthesis of target views from any viewpoint using volumetric rendering. NeRF’s representation has been applied to various tasks, including Simultaneous Localization and Mapping (SLAM) [7], scene reconstruction [20], scene segmentation [21], navigation [22], and manipulation [23].

NeRF-RL [24] treats the novel view synthesis task of NeRF as a proxy task, where the learned encoding network is directly used as feature input for reinforcement learning. NeRF-dy [25] uses NeRF as a perceptual decoder for the hidden states of a world model, training an additional dynamics estimation network to predict future state changes. NeRF2Real [26] learns real-world contexts by converting background meshes into a simulator, and trains robots to perform visual navigation, obstacle avoidance, and ball-handling tasks. However, the training speed of Vanilla NeRF has consistently been a bottleneck limiting its further deployment in practical applications.

3D GS [27] is an explicit radiance field method that directly updates the attributes of each 3D Gaussian component to optimize scene representation. 3D GS employs a splatting technique for rendering, and achieve extremely fast training efficiency through CUDA parallel technology. Moreover, compared to the implicit representation of NeRF, the explicit representation facilitates tracking dynamic scene modeling and editing scene content.

ManiGaussian [28] uses 3D GS as a dynamic attribute encoder for the scene, encoding spatiotemporal dynamic features of the scene as input for reinforcement learning. Quach et al. [29] combine GS with Liquid networks for real-world drone flight navigation tasks. They train flight strategies using imitation learning in a simulator and then deploy them in the real world.

In contrast to NeRF2Real [26], utilizes the images from the MuJoCo simulator for texturing the foreground objects.

We model each foreground object and use GS to edit the representation of the physical interactions with these foreground objects. Unlike the method designed by Quach et al. [29], which trains drone navigation for target-oriented tasks without involving complex interactions, our approach involves robotic arm manipulation tasks with complex interactions.

III. METHODS

The proposed framework aims to harness the potential of high-fidelity 3D GS models in sim2real for robot action training tasks. In this paper, we focus on manipulation tasks for robotic arms. As shown in Fig. 1, the overall framework is divided into two parts: real2sim and sim2real. In real2sim stage, we collect image data $\{\mathbf{I}_k\}$ in real-world operational scenarios, where \mathbf{I}_k represent the image sequences of the k -th object or background in the scenarios. We will model both the geometry and appearance of the scene to build a simulation environment for the manipulation task. In sim2real stage, we use visual perception and deep reinforcement learning to train a policy network, and directly transfer the policy to the real world.

A. Real2Sim: Building simulator with soft mesh binding GS

To obtain a realistic training simulation environment, we use consumer-grade cameras to capture 2D image data \mathbf{I}_k of desktop-level operating platforms. Our goal is to model a geometrically accurate and texture-realistic simulation model for training operational tasks. More specifically, we use mesh models $\{\mathbf{M}_k\}$ to represent the accurate geometric information, and Gaussian sets $\mathbf{G}_k = \{\mathbf{g}_k^i\}$ for high-quality texture. Below, we sequentially describe the steps to construct the Simulator with GS renderer.

1) *Real-world Data Preparing*: We use a monocular camera or mobile phone to capture a 1-2 minute video of the target object on the experimental platform. We select approximately 200 keyframes from the video and use COLMAP [30] to obtain the camera’s internal and external parameters for each frame. When modeling the object, image segmentation algorithm is also needed for extracting the target object. Many high-performance off-the-shelf segmenters are available, but we choose SAM-track [31] for efficient object segmentation.

To complete the GS model reconstruction for the simulator, it is also necessary to pre-model a geometrically accurate mesh model as a prior model for GS. Here we consider a classic and stable open-source package openMVS to obtain the corresponding mesh model.

2) *Real2Sim modeling by soft mesh binding GS*: With the object mesh, we can define Gaussian units within triangular faces as in GaMeS [9], a method that binds Gaussians onto the surface of meshes, and optimizes their properties through multi-view consistency. Vanilla GS [27] optimizes the attribute parameters of Gaussian units located at each point cloud position, where $\theta^i = (\mu^i, r^i, s^i, \sigma^i, c^i)$ denotes the position, rotation, scale, opacity, and color of the i -th Gaussian unit \mathbf{g}^i , respectively. To achieve controllable geometric editing effects, GaMeS [9] constrains Gaussian

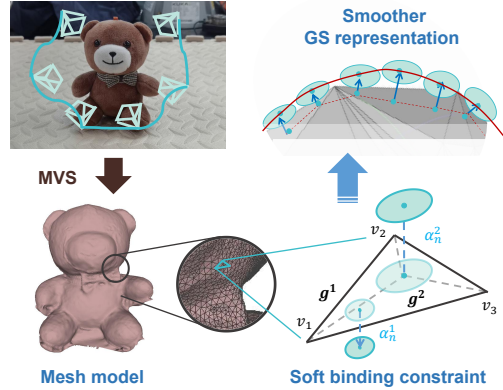


Fig. 2. Mesh-based GS Reconstruction with Soft Binding Constraints: Releasing the hard constraints of GaMeS [9] in the normal direction for smoother and more flexible object surfaces.

units within the triangular mesh of the object surface, using the mean vector as the convex combination of the mesh vertices to establish the positional relationship between the Gaussian unit and the three vertices of the triangular mesh:

$$\mu^i(\alpha_1^i, \alpha_2^i, \alpha_3^i) = \alpha_1^i \mathbf{v}_1 + \alpha_2^i \mathbf{v}_2 + \alpha_3^i \mathbf{v}_3, \quad (1)$$

here, $\mathbf{v}_1, \mathbf{v}_2, \mathbf{v}_3$ represents the triangular mesh vertex positions, $\alpha_1^i, \alpha_2^i, \alpha_3^i$ are learnable positional weight parameters for \mathbf{g}^i . However, we observe that this approach of enforced mesh-GS binding would diminish the flexibility of 3D Gaussians, limiting the optimization space of Gaussian units when the mesh model is not sufficiently fine or accurate, introducing certain undesirable defects.

To address this, we propose a soft mesh binding method, which builds on the rigid mesh binding of GaMeS [9] by relaxing the enforced hard binding and instead using a soft binding constraint to establish the association between mesh model elements and Gaussian units. We introduce a component along the normal direction into the mean vector of positions, specifically:

$$\mu^i(\alpha_1^i, \alpha_2^i, \alpha_3^i, \alpha_n^i) = \alpha_1^i \mathbf{v}_1 + \alpha_2^i \mathbf{v}_2 + \alpha_3^i \mathbf{v}_3 + \alpha_n^i \mathbf{v}_n, \quad (2)$$

here, α_n^i is a learnable weight parameter ranging in $[-1, 1]$, and \mathbf{v}_n is the normal vector. As shown in Fig. 2, our method allows the Gaussian units within the mesh to float within a certain range along the normal vector. This flexibility in Gaussian unit optimization could bring a smoother distribution of Gaussian units on the object’s surface. Ultimately, the algorithm not only ensures that the Gaussian model can still accurately represent the geometric structure of the scene but also offers some tolerance and refinement space, providing the possibility to handle non-rigid objects.

3) *Physic Dynamics-Based GS Editing*: We combine the dynamic simulation results from the simulator with real-time Gaussian model updates and render views to ensure that the visual representation follows the entire physical change process. We first use RANSAC plane regression and manual alignment methods to align GS models with mesh models in the simulator, and set the initial position of the GS model.

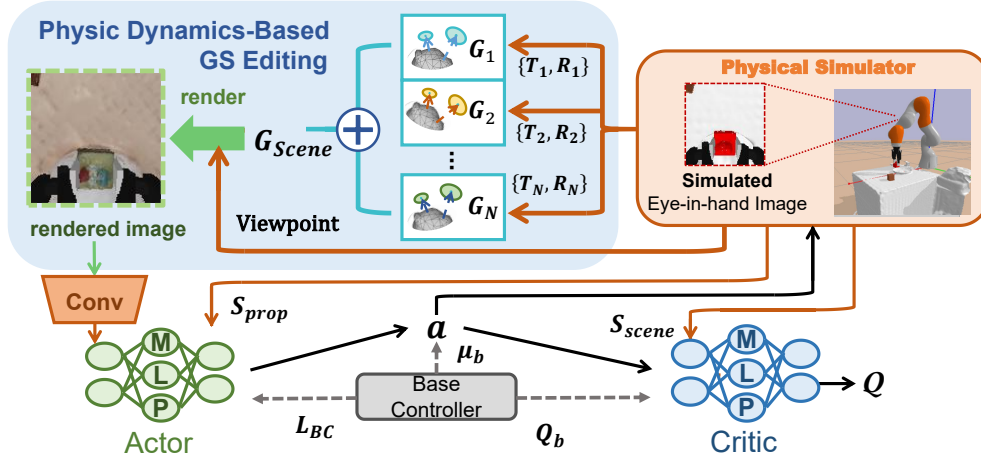


Fig. 3. Manipulation Policy Training: Converting physical simulation dynamics signals into rotation and translation signals for GS editing, synchronizing GS model updates, and using first-person perspective scenes rendered by GS models as input for an actor-critic RL network to learn the manipulation policy.

TABLE I

COMPARISON OF SUCCESS RATES FOR SMALL-CUBE AND BEAR GRASPING EXPERIMENTS BETWEEN RL-GSBRIDGE AND RL-SIM: **BOLD** INDICATES THE BETTER RESULT BETWEEN THE TWO METHODS, WITH VALUES IN PARENTHESES REPRESENTING THE CHANGE IN SUCCESS RATE WHEN TRANSFERRED TO THE REAL WORLD RELATIVE TO THE SIMULATION ENVIRONMENT. ($\downarrow XX\%$) INDICATES A DECREASE OF $XX\%$, AND ($\uparrow XX\%$) INDICATES AN INCREASE OF $XX\%$.

Object	Small-cube		Bear	
	Sim	Real	Sim	Real
RL-sim	96.88	12.50 ($\downarrow 87\%$)	93.75	25.00 ($\downarrow 73\%$)
RL-GSBridge	96.88	96.88	87.50	100.00 ($\uparrow 14\%$)

With the aligned initial model, we read the real-time pose changes of objects in the operational scene from the simulator. For the k -th object, We acquire the rotation quaternion q_k and the homogeneous transformation matrix \mathbf{T}_k in the world coordinate system. Given Gaussian parameters $\theta_k^i = (\mu_k^i, r_k^i, s_k^i, \sigma_k^i, c_k^i)$, The editing process of each Gaussian \mathbf{g}_k^i in the Gaussian set \mathbf{G}_k could be formulated as:

$$\mu_k^i = \mathbf{T}_k \mu_k^i, \quad r_k^i = q_k \times r_k^i. \quad (3)$$

After applying the correspondence transformations to all object models, we concat the Gaussian sets to acquire the Gaussian model of the whole scene \mathbf{G}_{scene} . Then we use rasterization to render \mathbf{G}_{scene} , obtaining the synchronized edited rendering view.

B. Sim2Real: Train in simulation with physic dynamics-based GS renderer and zero-shot transfer to reality

We use Pybullet [32] as the simulation training platform and employ the SAC (Soft Actor-Critic) [33] algorithm for policy learning. The SAC is an offline policy algorithm belonging to maximum entropy RL, which consists of two critic networks, $Q_{\phi,1}(s,a)$ and $Q_{\phi,2}(s,a)$, and one actor

network, $\pi_{\theta}(s)$. For the sampled set B from the replay buffer, the update loss of critic is defined as:

$$Loss_{critic} = \frac{1}{|B|} \sum_{(s_t, a_t, r_{t+1}, s_{t+1}) \in B} (y_t - Q_{\phi,j}(s_t, a_t))^2, \quad (4)$$

here, $(s_t, a_t, r_{t+1}, s_{t+1})$ is a tuple belong to B , the y_t is calculated by target Q networks $Q_{\bar{\phi},j}$:

$$y_t = r_t + \gamma (\min_{j=1,2} Q_{\bar{\phi},j}(s_{t+1}, a_{t+1}) - \alpha \log \pi_{\theta}(a_{t+1}|s_{t+1})). \quad (5)$$

For continuous action spaces, the SAC policy network π_{θ} outputs actions following Gaussian distribution. The update loss of actor is defined as:

$$Loss_{actor} = \frac{1}{|B|} \sum_{(s_t, a_t, r_{t+1}, s_{t+1}) \in B} (\alpha \log \pi_{\theta}(\tilde{a}_t | s_t) - \min_{j=1,2} Q_{\phi,j}(s_t, \tilde{a}_t)), \quad (6)$$

where \tilde{a}_t is sampled using the reparameterization trick, i.e., $a_t = f_{\theta}(\epsilon_t; s_t)$, ϵ is Gaussian random noise. In practical implementation, we set: $f_{\theta} = \tanh(\mu_{\theta}(s_t) + \sigma_{\theta}(s_t) \odot \epsilon_t)$.

Building on SAC and referencing DDPGwB [34], we propose SACwB, and introduce a lightly designed baseline controller incorporating artificial experience to guide the policy. This approach avoids complex reward designs while eliminating ineffective action spaces.

In SACwB, the agent executes actions from the baseline controller with probability λ and selects the best option between the baseline controller's and the actor's outputs with probability $1 - \lambda$, the objective is typically defined as:

$$y_t = r_t + \gamma \max \left(\left(\min_{j=1,2} Q_{\bar{\phi},j}(s_{t+1}, a_{t+1}) - \alpha \log \pi_{\theta}(a_{t+1}|s_{t+1}) \right), \left(\min_{j=1,2} Q_{\bar{\phi},j}(s_{t+1}, \mu_b(s_{t+1})) - \alpha \log \pi_{\theta}(\mu_b(s_{t+1})|s_{t+1}) \right) \right). \quad (7)$$

In the supervision of the actor network, we introduce an additional behavior clone loss L_{bc} in Equation 6 to supervise

TABLE II
SIM2REAL RESULTS FOR THE GRASPING TASK IN VARIOUS COMPLEX MANIPULATION SCENARIOS WITH RL-GSBRIDGE.

Object (Background)	Cake (Foam pad)		Banana (Foam pad)		Small-cube (Tablecloth)		Cake (Tablecloth)		Banana (Tablecloth)		Bear (Tablecloth)	
	Sim	Real	Sim	Real	Sim	Real	Sim	Real	Sim	Real	Sim	Real
Success rate (%)	100.00	100.00	100.00	93.75 (↓6%)	96.88	87.50 (↓10%)	100.00	93.75 (↓6%)	100.00	96.88 (↓3%)	87.50	75.00 (↓14%)



Fig. 4. Comparison of sim-to-real behavior consistency between RL-GSBRIDGE and RL-sim.

TABLE III
THE SIM2REAL RESULT FOR THE PICK AND PLACE TASK.

Object	Cake & Plate	
	Sim	Real
Success rate (%)	68.75	71.87 (↑4%)

the mean of the actions output by the actor using base controller actions, with the probability λ :

$$L_{bc} = \|\mu_{\theta}(s) - \mu_b(s)\|^2, \quad (8)$$

and with the probability $1 - \lambda$:

$$L_{bc} = \left\| \mu_{\theta}(s) - \mu \left| \arg \max_{j=1,2} Q_{\bar{\phi},j}(s, \mu_{\theta}(s)) \right. \right\|^2, \quad (9)$$

here, λ is the decay factor, which gradually approaches 0 as training progresses.

The whole training pipeline in the simulator with physic dynamics-based GS renderer is shown in Fig. 3. The RL algorithm provides executable actions to the physics simulator, which will provide state information for actor and critic learning. The GS renderer simultaneously renders the realistic images by physic dynamics-based GS rendering, serving as observation input to the actor network. We rely solely on the first-person perspective 2D image and proprioceptive state of the robotic arm, considering several advantages as described in [35]. To enhance sim2real robustness, we add random noise to the rendered images of the GS model and randomly alter certain image attribute parameters during training for environment challenges.

After policy training in the simulator, we use ROS as the communication medium, with the actual first-person perspective camera observations of the environment serving as input to the policy inference network. The trained policy network then outputs executable actions.

IV. EXPERIMENTS

A. Experiment Setup

1) *Robot Platform*: We use a KUKA iiwa robot arm paired with a Robotiq 2F-140 gripper as the platform. The Intel RealSense D435i camera fixed on the robot arm captures the RGB images from the first-person perspective.

2) *Tasks*: As shown in Fig. 1, we design two types of tasks from the robot’s first-person perspective: grasping and pick-and-place operations.

For grasping, the robot grasps a target object and lifts it up. The initial positions of the objects are randomized within a 30×30 cm section. We use Small_cube, Cake, Banana, and Bear as objects. As for the operation platform, we use a foam pad with and without a tablecloth as two different backgrounds. Success is considered when the object is lifted 10 cm above the table.

For pick-and-place tasks, the robotic arm pick up the cake model and place it on a plate. The position of the cake is set similarly as described in the grasping task. The plate is placed in a fixed position on the foam pad. Success is considered when the cake is placed on the plate.

3) *Setup*: For each task, we conduct both the simulation and the real world. During testing, we divide the 30×30 cm section into four quadrants. For each task, we test the policy across a fixed number of positions in each quadrant to calculate the success rate.

4) *Baseline*: To demonstrate that our method effectively reduces sim2real gap, we conduct a baseline experiment called RL-sim: using the same learning method but training directly on images rendered from mesh models shaded in the PyBullet simulator. We select two representative and easily shaded objects: the Small-cube and Bear. Grasping experiments for RL-sim are conducted on a foam pad.

B. Experiment Results

1) *Grasping*: In Table I, we compare the grasping performance of RL strategies trained with the baseline (RL-

TABLE IV

OUR SOFT BINDING CONSTRAINT RECONSTRUCTION METHOD COMPARED WITH GaMeS [9] ON MULTIPLE FOREGROUND OBJECTS AND BACKGROUND RENDERING METRICS. SSIM IS SCALE STRUCTURAL SIMILARITY INDEX. PSNR IS PEAK SIGNAL-TO-NOISE RATIO. LPIPS IS LEARNED PERCEPTUAL IMAGE PATCH SIMILARITY.

	Banana		Bear		Cake		Small-cube		Bg (raw)		Bg (tablecloth)		Bg (plate)	
	Ours	GaMeS	Ours	GaMeS	Ours	GaMeS	Ours	GaMeS	Ours	GaMeS	Ours	GaMeS	Ours	GaMeS
SSIM \uparrow	0.989	0.894	0.964	0.956	0.975	0.964	0.989	0.989	0.944	0.939	0.781	0.776	0.776	0.756
PSNR \uparrow	35.46	26.53	29.82	28.18	33.38	30.73	37.18	36.64	28.40	27.32	22.88	21.86	21.86	20.80
LPIPS \downarrow	0.026	0.049	0.034	0.040	0.066	0.079	0.012	0.012	0.144	0.149	0.248	0.308	0.308	0.311

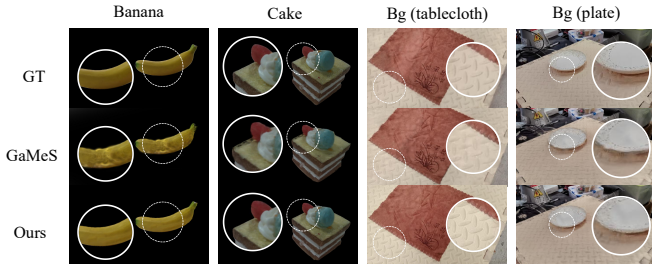


Fig. 5. Our soft binding constraint reconstruction method compared with GaMeS [9] on two foreground objects and two backgrounds.

sim) and RL-GSBridge in both simulation and real environments. For both the Small-cube with structured geometry and simple textures and the Bear with unstructured geometry and complex textures, RL-sim shows a significant success rate drop when transferring to real scenarios (an average decrease of 80%) due to substantial visual discrepancies. In contrast, RL-GSBridge not only avoids a success rate drop but also improves it in the Bear grasping scenario (an increase of 14.28%). Our analysis suggests that the rough geometry of unstructured objects in simulation (e.g., unintended protrusions or gaps) would increase the difficulty of completing tasks.

Table II shows that RL-GSBridge experiences an average drop of 6.6% of the success rate in sim-to-real transfer across various complex test scenarios, including diverse objects and desktop backgrounds. This demonstrates that the integration of the physic dynamics-based GS rendering effectively bridges the perception gap between simulation and real environments, maintaining stable strategy transfer success rates across a range of scenarios. Additionally, we observe a noticeable decrease in success rates for the Bear in the Tablecloth background scenario, both in simulation and real environments. The primary reason for this drop is the choice of a brown tablecloth, which has similar texture features to the brown toy bear, causing interference with the strategy network’s decision-making process.

2) *Pick-and-Place*: As shown in Table III, we test RL-GSBridge’s sim-to-real performance in a pick-and-place task where a cake is placed onto a plate. The results indicate a 4.54% increase in success rate in real environments. Our analysis suggests that this improvement is due to the differences in perception between simulation and reality. In the simulation, even minor excess contacts during the cake



Fig. 6. The editing capability on non-rigid objects of our soft binding constraint GS modeling method.

placement process are considered as task failures. In contrast, in real environments, some contacts that do not affect the overall task can be tolerated, leading to a higher success rate as the task is ultimately completed successfully.

3) *Comparison of Sim&Real Behavior Consistency*: In Fig. 4, we compare the behavior of the robotic arm in the simulator and in real scenarios. With the same initialization settings, RL-GSBridge exhibits behavior highly consistent with the simulation tests during the grasping process, including first-person perspective perception and the arm’s process posture, whereas RL-sim without the GS model shows significant differences.

4) *GS Rendering results of different Mesh Binding approach*: In Table IV, we compare the performance of GaMeS [9] and our soft binding constraints GS modeling method under the setting scenarios and achieve the SOTA performance. Furthermore, Fig. 5 shows that our method obtains fewer artifacts and more detailed texture rendering. As a supplement, in Fig. 6, our soft binding constraint GS modeling method achieves consistent results in editing a non-rigid toy bear, which is beneficial for learning manipulation strategies for non-rigid objects.

V. CONCLUSIONS

We propose RL-GSBridge, a RL framework for sim-to-real applications. As an attempt to apply the recently successful radiance field reconstruction methods to robotics, RL-GSBridge has shown promising sim-to-real success rates in desktop-level tasks from the robotic arm’s first-person perspective. This motivates us to explore future directions, such as applying and improving our method on more diverse platforms and tackling more complex tasks. For instance, RL-GSBridge currently lacks generalization capabilities, and developing the ability for adaptive learning is a promising area of exploration. We hope RL-GSBridge will encourage more attempts to apply radiance field reconstruction methods in robotics.

REFERENCES

- [1] W. Zhao, J. P. Qeralta, L. Qingqing, and T. Westerlund, "Towards closing the sim-to-real gap in collaborative multi-robot deep reinforcement learning," in *2020 5th International conference on robotics and automation engineering (ICRAE)*. IEEE, 2020, pp. 7–12.
- [2] F. Muratore, C. Eilers, M. Gienger, and J. Peters, "Bayesian domain randomization for sim-to-real transfer," *arXiv preprint arXiv:2003.02471*, 2020.
- [3] K. Arndt, M. Hazara, A. Ghadirzadeh, and V. Kyrki, "Meta reinforcement learning for sim-to-real domain adaptation," in *2020 IEEE international conference on robotics and automation (ICRA)*. IEEE, 2020, pp. 2725–2731.
- [4] R. Traoré, H. Caselles-Dupré, T. Lesort, T. Sun, N. Díaz-Rodríguez, and D. Filliat, "Continual reinforcement learning deployed in real-life using policy distillation and sim2real transfer," *arXiv preprint arXiv:1906.04452*, 2019.
- [5] B. Mildenhall, P. P. Srinivasan, M. Tancik, J. T. Barron, R. Ramamoorthi, and R. Ng, "Nerf: Representing scenes as neural radiance fields for view synthesis," in *ECCV*, 2020.
- [6] K. Zhang, G. Riegler, N. Snavely, and V. Koltun, "Nerf++: Analyzing and improving neural radiance fields," *arXiv preprint arXiv:2010.07492*, 2020.
- [7] Z. Zhu, S. Peng, V. Larsson, W. Xu, H. Bao, Z. Cui, M. R. Oswald, and M. Pollefeys, "Nice-slam: Neural implicit scalable encoding for slam," in *CVPR*, 2022, pp. 12 786–12 796.
- [8] S. Zhu, G. Wang, H. Blum, J. Liu, L. Song, M. Pollefeys, and H. Wang, "Sni-slam: Semantic neural implicit slam," *CVPR*, 2024.
- [9] J. Waczyńska, P. Borycki, S. Tadeja, J. Tabor, and P. Spurek, "Games: Mesh-based adapting and modification of gaussian splatting," *arXiv preprint arXiv:2402.01459*, 2024.
- [10] V. François-Lavet, P. Henderson, R. Islam, M. G. Bellemare, J. Pineau, et al., "An introduction to deep reinforcement learning," *Foundations and Trends® in Machine Learning*, vol. 11, no. 3-4, pp. 219–354, 2018.
- [11] D. Silver, A. Huang, C. J. Maddison, A. Guez, L. Sifre, G. Van Den Driessche, J. Schrittwieser, I. Antonoglou, V. Panneershelvam, M. Lanctot, et al., "Mastering the game of go with deep neural networks and tree search," *nature*, vol. 529, no. 7587, pp. 484–489, 2016.
- [12] Y. Deng, F. Bao, Y. Kong, Z. Ren, and Q. Dai, "Deep direct reinforcement learning for financial signal representation and trading," *IEEE transactions on neural networks and learning systems*, vol. 28, no. 3, pp. 653–664, 2016.
- [13] X. Pan, Y. You, Z. Wang, and C. Lu, "Virtual to real reinforcement learning for autonomous driving," *arXiv preprint arXiv:1704.03952*, 2017.
- [14] L. Pinto, M. Andrychowicz, P. Welinder, W. Zaremba, and P. Abbeel, "Asymmetric actor critic for image-based robot learning," *arXiv preprint arXiv:1710.06542*, 2017.
- [15] Y. Liu, W. Chen, Y. Bai, J. Luo, X. Song, K. Jiang, Z. Li, G. Zhao, J. Lin, G. Li, et al., "Aligning cyber space with physical world: A comprehensive survey on embodied ai," *arXiv preprint arXiv:2407.06886*, 2024.
- [16] J. Tobin, R. Fong, A. Ray, J. Schneider, W. Zaremba, and P. Abbeel, "Domain randomization for transferring deep neural networks from simulation to the real world," in *2017 IEEE/RSJ international conference on intelligent robots and systems (IROS)*. IEEE, 2017, pp. 23–30.
- [17] K. Bousmalis, A. Irpan, P. Wohlhart, Y. Bai, M. Kelcey, M. Kalakrishnan, L. Downs, J. Ibarz, P. Pastor, K. Konolige, et al., "Using simulation and domain adaptation to improve efficiency of deep robotic grasping," in *2018 IEEE international conference on robotics and automation (ICRA)*. IEEE, 2018, pp. 4243–4250.
- [18] J. X. Wang, Z. Kurth-Nelson, D. Tirumala, H. Soyer, J. Z. Leibo, R. Munos, C. Blundell, D. Kumaran, and M. Botvinick, "Learning to reinforcement learn," *arXiv preprint arXiv:1611.05763*, 2016.
- [19] A. A. Rusu, S. G. Colmenarejo, C. Gulcehre, G. Desjardins, J. Kirkpatrick, R. Pascanu, V. Mnih, K. Kavukcuoglu, and R. Hadsell, "Policy distillation," *arXiv preprint arXiv:1511.06295*, 2015.
- [20] Z. Yu, S. Peng, M. Niemeyer, T. Sattler, and A. Geiger, "Monosdf: Exploring monocular geometric cues for neural implicit surface reconstruction," *NeurIPS*, pp. 25 018–25 032, 2022.
- [21] S. Zhi, T. Laidlow, S. Leutenegger, and A. J. Davison, "In-place scene labelling and understanding with implicit scene representation," in *ICCV*, 2021, pp. 15 838–15 847.
- [22] M. Adamkiewicz, T. Chen, A. Caccavale, R. Gardner, P. Culbertson, J. Bohg, and M. Schwager, "Vision-only robot navigation in a neural radiance world," *RA-L*, pp. 4606–4613, 2022.
- [23] Q. Dai, Y. Zhu, Y. Geng, C. Ruan, J. Zhang, and H. Wang, "Grasprerf: multiview-based 6-dof grasp detection for transparent and specular objects using generalizable nerf," in *ICRA*, 2023, pp. 1757–1763.
- [24] D. Driess, I. Schubert, P. Florence, Y. Li, and M. Toussaint, "Reinforcement learning with neural radiance fields," *NeurIPS*, 2022.
- [25] Y. Li, S. Li, V. Sitzmann, P. Agrawal, and A. Torralba, "3d neural scene representations for visuomotor control," in *CoRL*, 2022, pp. 112–123.
- [26] A. Byravan, J. Humplik, L. Hasenclever, A. Brussee, F. Nori, T. Haarnoja, B. Moran, S. Bohez, F. Sadeghi, B. Vujatovic, et al., "Nerf2real: Sim2real transfer of vision-guided bipedal motion skills using neural radiance fields," in *ICRA*, 2023, pp. 9362–9369.
- [27] B. Kerbl, G. Kopanas, T. Leimkuehler, and G. Drettakis, "3d gaussian splatting for real-time radiance field rendering," *ACM Trans. Graph.*, vol. 42, no. 4, 2023.
- [28] G. Lu, S. Zhang, Z. Wang, C. Liu, J. Lu, and Y. Tang, "Manigaussian: Dynamic gaussian splatting for multi-task robotic manipulation," *arXiv preprint arXiv:2403.08321*, 2024.
- [29] A. Quach, M. Chahine, A. Amini, R. Hasani, and D. Rus, "Gaussian splatting to real world flight navigation transfer with liquid networks," *arXiv preprint arXiv:2406.15149*, 2024.
- [30] J. L. Schönberger and J.-M. Frahm, "Structure-from-motion revisited," in *Conference on Computer Vision and Pattern Recognition (CVPR)*, 2016.
- [31] Y. Cheng, L. Li, Y. Xu, X. Li, Z. Yang, W. Wang, and Y. Yang, "Segment and track anything," *arXiv preprint arXiv:2305.06558*, 2023.
- [32] E. Coumans and Y. Bai, "Pybullet, a python module for physics simulation for games, robotics and machine learning," 2016.
- [33] T. Haarnoja, A. Zhou, P. Abbeel, and S. Levine, "Soft actor-critic: Off-policy maximum entropy deep reinforcement learning with a stochastic actor," in *International conference on machine learning*. PMLR, 2018, pp. 1861–1870.
- [34] G. Wang, M. Xin, W. Wu, Z. Liu, and H. Wang, "Learning of long-horizon sparse-reward robotic manipulator tasks with base controllers," *IEEE Transactions on Neural Networks and Learning Systems*, vol. 35, no. 3, pp. 4072–4081, 2022.
- [35] K. Hsu, M. J. Kim, R. Rafailov, J. Wu, and C. Finn, "Vision-based manipulators need to also see from their hands," in *International Conference on Learning Representations*, 2021.